

A NOVEL STRESS-STRAIN MICROPROBE FOR NONDESTRUCTIVE EVALUATION
OF MECHANICAL PROPERTIES OF MATERIALS

Fahmy M. Haggag,¹ K. Linga Murty²

¹Advanced Technology Corporation, 115 Clemson Dr., Oak Ridge TN 37830

²North Carolina State University, Raleigh, North Carolina 27695-7909

Abstract

A novel portable/in-situ Stress-Strain Microprobe (SSM) system was used to measure true-stress/true-plastic-strain behavior of several metallic materials, welds, and their heat-affected-zones (HAZs) in various metallurgical and damage conditions. The automated ball indentation (ABI) technique of the SSM system is based on strain-controlled multiple indentations (at a single penetration location) of a polished surface by a spherical indenter (e.g. 0.25 to 1.57 mm diameter) and the indentation depth is progressively increased to a maximum user-specified limit with intermediate partial unloadings. Recent advances include single cycle method and development of *in-situ* probe. The technique permits measurement of yield strength, stress-strain curve, strength coefficient, and strain-hardening-exponent (uniform ductility). Tests were performed on carbon steels, stainless steels, nickel alloys, aluminum alloys, Zircalloys, electronic soldering materials, etc. Numerous ABI tests were also conducted on several nuclear pressure vessel steels (NPVSs) in the unirradiated, neutron irradiated, and post-irradiated thermally annealed conditions. For all these test materials and conditions, the ABI-derived results were in very good agreement with those from conventional standard test methods.

Introduction

A fundamental requirement to properly assess the degradation and remaining life of structures in various applications is the development of techniques to characterize the mechanical and fracture properties on components of various structures. While destructive test techniques of specimens made from materials of which these structures were constructed do provide relevant data, direct measurement preferably using nondestructive techniques on the *real* structures is desirable for reliable assessment of the safety of these structures. Another important criterion is that the technique should be capable of yielding these data using minimal amount of material so that gradient properties in welds and their heat-affected-zones (HAZ) can be evaluated. One such technique is the Automated Ball Indentation (ABI) which has been demonstrated to yield the stress-strain behaviors of many structural metals such as ferritic steels, stainless steels, aluminum alloys, electronic solders, etc. While the idea of ball indentation is not new [1], the uniqueness of ABI lies in the fact that this technique does not require post measurement of the diameter of indentation using elaborate profilometry, optical interferometry,

etc., which render the traditional methodology unsuitable for online monitoring of the mechanical properties of structures in-service. Based on this principle, a portable/in-situ stress-strain microprobe (SSM) system was developed recently by Advanced Technology Corporation (ATC) to test minimal material and determine several mechanical properties (e.g. yield strength, flow properties, strain-hardening exponent, strength coefficient) of metallic structures including their welds and heat-affected zones [2]. The SSM system and test methods are based on well demonstrated and accepted physical and mathematical relationships which govern metal behavior under multiaxial indentation loading [2,3]. A summary of the automated ball indentation (ABI) technique is given in reference 2 while more details may be found elsewhere [4 6].

We applied this ABI technique to characterize the stress-strain characteristics of various materials using SSM and to compare them with the tensile and creep tests on the same material. ABI is a relatively simple, rapid (~ few minutes) and nondestructive technique, requires small amounts of material with essentially no specimen preparation, and can be adopted for *in-situ* testing on *real* structures. Extensions of this methodology can be made for high temperature studies as well as indentation fatigue, fracture and creep. We describe here the ABI experimental and analytical procedures along with sample results (on specimens and components) using a commercially available SSM system. In addition, results using a new single-cycle ABI test procedure, developed for high strain-rate testing and continuous stress-strain measurement, are provided for electronic solder materials (Sn5%Sb). Potential future research areas for utilizing the SSM system to determine fatigue and creep damage as well as to measure residual stresses are briefly described in this paper.

Stress-Strain Microprobe (SSM)

The microprobe system currently utilizes an electro-mechanically-driven indenter, high resolution penetration transducer and load cell, a personal computer (PC), a 16-bit data acquisition/control unit, and a copyrighted ABI software. Automation of the test, where a PC and a test controller were used in innovative ways to control the test (including real-time graphics and digital display of load-depth test data) as well as to analyze test data (including tabulated summary and macro-generated plots), made it accurate and highly reproducible. Figure 1 shows the overall view (a) of the SSM along with a close-up of the indenter and the LVDT. The technique involves indenting a specimen with a tungsten carbide sphere (of appropriate diameter varying from 0.254

mm to 1.575 mm) while monitoring the load versus depth of penetration using an on-line load cell and an LVDT respectively. The ball indenter is electro-mechanically-driven at a constant speed and multiple unloadings were performed to evaluate the plastic indentation depth. Unique PC software was developed to evaluate the plastic stress and strain using elastic and plastic analyses. These innovative techniques eliminated the cumbersome post indentation measurement of the indentation diameter at specific loads. Recent extensions include single cycle tests with no intermediate partial unloadings. Such tests are required for high strain-rate testing and continuous stress-strain measurement.

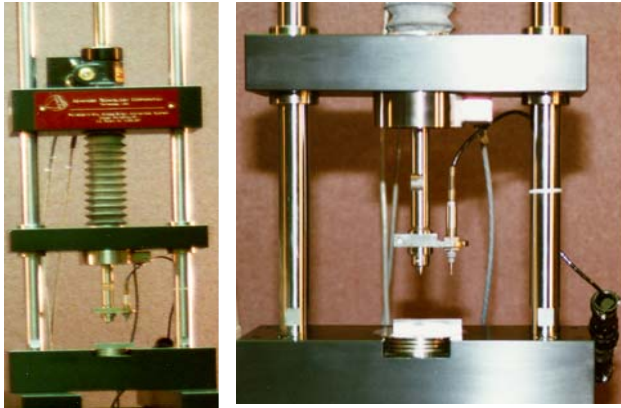


Figure 1
SSM Machine (left) and Close-Up (right)
Showing the Indenter and LVDT

One of the unique features of the system is its portability and capabilities for tests on *real* structures. Figure 2a shows in-situ SSM configuration that was used successfully to test a 100-mm outer diameter 347 SS pipe containing a circumferential weld. In addition, other testing heads such as magnetic holders were also attempted; Fig. 2b depicts such an arrangement on a block of pressure vessel (PV) steel.



Figure 2a
SSM on a 347 Stainless
Steel Pipe



Figure 2b
SSM on a Steel Block with
Magnetic Attachment

ABI Data Analyses

A typical indentation load-depth curve obtained using 1.57 mm ball from an *in-situ* ABI test on the HAZ in a circumferentially welded 347 SS pipe (shown in Fig. 2a) is

reproduced in Fig. 3a where the standard seven loading-unloading cycles were used. All tests were completely computer controlled and the system software package lists the various input parameters along with the results for the yield strength, work-hardening parameters, tensile strength as well as Brinell hardness in addition to the plastic true stresses and strains for the seven points. The reason for the approximately linear relation of indentation load versus depth is because of the doubly nonlinear processes occurring in opposite directions (i.e. the nonlinear increase of load versus depth due to the spherical geometry of the ball indenter is being offset by the power-law work-hardening behavior of the metallic test material). Hence, ABI tests do not exhibit the traditional segmented behavior (linear elastic followed by nonlinear / work-hardening) of the tensile load-displacement data.

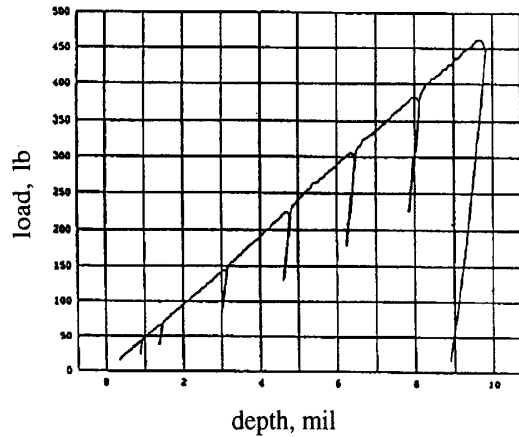


Figure 3a
In-situ ABI test - Load versus Depth

A brief summary of the relevant equations used in the derivation of the flow properties is included here while the details may be found in various references [1 - 3]. The primary information obtained from ABI tests comprises the indentation load (P) and the depth/height of penetration (h_p). The system software calculates the plastic strain while the flow stresses are evaluated using elastic and plastic analyses. The true plastic strain is given by [1],

$$\epsilon_p = 0.2 \frac{d_p}{D} \quad (1)$$

where d_p and D are the *plastic* indentation diameter and diameter of indenter respectively. The corresponding flow stress is calculated using [2],

$$\sigma_i = \frac{4P}{\pi d_p^2 \delta} \quad (2)$$

where σ_i is the true indentation stress, P is indentation load and δ is a parameter which depends on the system compliance and indentation stress with a value between 1.12 and $2.87\alpha_m$; α_m is known as the constraint factor which depends on the strain rate sensitivity and biaxial hardening, with a value of unity for strain-rate insensitive materials. The plastic indentation depth, d_p , is given by,

$$d_p = \sqrt[3]{2.735 P \left(\frac{1}{E_i} + \frac{1}{E_s} \right) D \left\{ \frac{h_p^2 + 0.25d_p^2}{h_p^2 + 0.25d_p^2 - h_p D} \right\}} \quad (3)$$

Here, E_i and E_s represent the elastic moduli of the indenter and the specimen respectively. As we note here, the parameter d_p appears in both the left and right hand terms and thus an iterative solution is sought which the software of the system has the capability to evaluate. The plastic stress and strain can be related by the power law,

$$\sigma_{TS} = K \epsilon_p^{n'} \quad (4)$$

where K and n' are the strength coefficient and the strain-hardening parameter respectively. From the fact that the strain-hardening parameter, n' , is equal to the true uniform strain, one can evaluate the true tensile stress (σ_{TS}),

$$\sigma_{TS} = K (n')^{n'} \quad (5)$$

The ultimate tensile strength (engineering value) is then obtained from

$$UTS = K \left\{ \frac{n'}{e} \right\}^{n'} \quad (6)$$

In addition to the UTS, one often requires the yield strength which can also be obtained from the flow rule. However, it is found to be convenient to relate the indentation load and diameter through Meyer's coefficient (m'),

$$\frac{P}{d_i^2} = A \left\{ \frac{d_i}{D} \right\}^{m' - 2} \quad (7)$$

The constant A is a material parameter through which one may find the yield strength (σ_y),

$$\sigma_y = \beta_m A \quad (8)$$

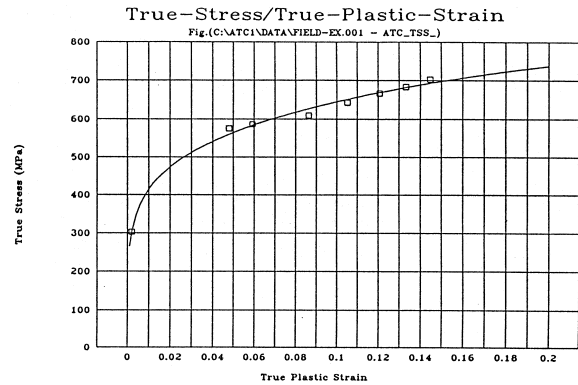
In this equation, β_m is a material-type constant (i.e., a single value of 0.2285 for carbon steels is applicable whether cold rolled, hot rolled, irradiated, etc.). Extensive correlations by Haggag et al [2 - 4] revealed good agreement between ABI and tensile data for many ferritic steels with essentially identical β_m value. Another factor that is derived from the ABI data and is a part of the system software is the Brinell hardness (BHN) obtained from,

$$BHN = \frac{2 P_{max}}{\pi D \left(D - \sqrt{D^2 - d_{max}^2} \right)} \quad (9)$$

It is clear from the above description that many useful mechanical property data can be obtained from ABI and extensive correlations have been made for many structural metals.

Figure 3b is the true stress versus true strain derived from the ABI data in Fig. 3a along with the total stress-strain curve fit. No direct comparison with tensile stress-strain data is possible here and such a comparison is shown in Fig. 4 for A533B steel which is commonly used in nuclear pressure vessels. We note an excellent agreement between ABI and tensile test results. Here, the ABI tests were performed on the shoulder portions of the tensile tested

specimens thereby eliminating any specimen-to-specimen scatter.



True Strain
Figure 3b

True σ - ϵ Curve for 347SS Weld Derived from ABI Data

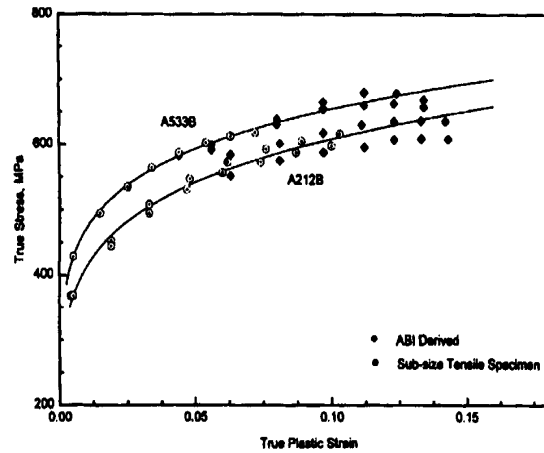


Figure 4

σ - ϵ Curves for A533B and A212B Steels

Results and Discussion

Ferritic Steels

While Fig. 4 shows the excellent correlation between tensile and ABI tests, such correlations were noted in other steels as well and we depict similar test results (Fig. 4) on A212B steel which finds extensive application as reactor support steels. It should be pointed out that the quality of the data is not affected by the surface finish. Druce et al [7] clearly demonstrated that identical ABI test data can be obtained on samples with a range of surface finishes from the original as-cut by silicon-carbide tool through various stages of metallographic finishes using 600-grade grit, 6 micron and 0.25 micron diamond polishes.

Weld and HAZs

SSM was used in testing laboratory specimens of a double-V weld from a high strength steel. The ABI test results at three test locations of the base metal (BM), heat-affected-zone (HAZ), and weld metal (Weld) are shown in Fig. 5. This figure

shows that the flow properties (true-stress/true-plastic-strain curve) of the HAZ is not necessarily bracketed by those from the BM and Weld on both sides of the HAZ material. It might be higher (Fig. 5) or lower than both of them. ABI tests performed on spot welds from 1020 mild steel weld (Fig. 6) do show that the flow properties (true-stress/true-plastic-strain curve) of the HAZ are bracketed by those from the BM and Weld on both sides of the HAZ material [8]. The nondestructive aspect of the ABI technique allows testing welded joints without the need to destructively machine miniature specimens which might also release residual stresses (generated from the welding procedure). Furthermore, the localized ABI testing allows examining very narrow and/or irregular geometry HAZ areas. The SSM system can be used in-situ to map-out gradients in the stress-strain behavior of welded structural components nondestructively. Hence, structural integrity and/or proper welding procedures and post-weld heat treatments can be evaluated.

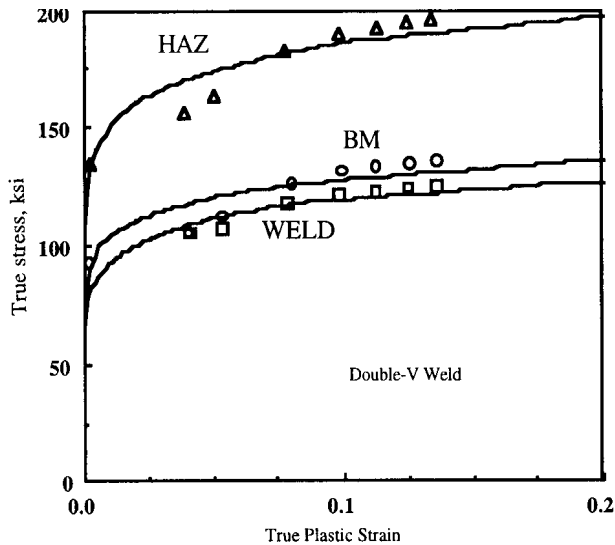


Figure 5
ABI σ - ϵ Curves on Base Metal (BM), Weld Metal (Weld) and Heat-Affected Zone (HAZ) of PV Steel

In-situ ABI Testing of Structural Components

Figures 2 and 3 clearly demonstrate the utility of SSM in assessing the mechanical properties of structures *in-situ*. The testing head of the portable/in-situ stress-strain microprobe system was clamped on the pipe using four 90° V-blocks as shown in Fig. 2. This mounting method allowed the testing head to be rotated 360° and clamped rigidly for ABI testing at any location of the weld, HAZ, or the base metal. A value of $B_m = 0.191$ (obtained from comparison with tensile test data) was used for all ABI tests on stainless steel samples and pipe materials. The results are summarized in Table 1.

These ABI test results show that the flow properties measured by the microprobe at three circumferential weld areas are in good agreement with each other and are consistently slightly lower than those at the base metal and the HAZ test locations. The above *in-situ* tests also successfully demonstrate the potential applicability of the microprobe system to nondestructively test welded pipes and pressure vessels in the petroleum, fossil and nuclear power plants, etc.

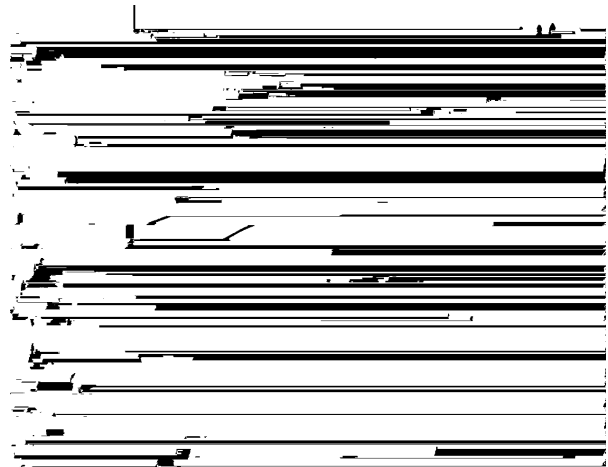


Figure 6
ABI σ - ϵ Curves on Base Metal (BM), Weld Metal (Weld) and Heat-Affected Zone (HAZ) of 1020 Mild Steel

Table 1
ABI Results on 347 SS Weld

Material	Flow Equation	Yield Strength MPa
Base Metal (347 SS)	$\sigma = 1097 \epsilon^{0.197}$	325
Weld Metal (308 SS)		
Location #1	$\sigma = 190 \epsilon^{0.198}$	283
Location #2	$\sigma = 920 \epsilon^{0.198}$	283
Location #3	$\sigma = 971 \epsilon^{0.198}$	300
HAZ	$\sigma = 1060 \epsilon^{0.191}$	331

Radiation and Post-Irradiation Thermal Annealing

The ABI technique was used to assess the degree of neutron-embrittlement damage and the percentage ductility recovery due to post-irradiation thermal annealing. Fig. 7 depicts the true stress-strain curves for A533B pressure vessel steel (Heavy Section Steel Technology (HSST) Plate 02) in four conditions [9]: unirradiated (as in Fig. 4), neutron irradiated to a fast fluence of 2×10^{19} n/cm², and two post-irradiated thermally-annealed conditions (for 604,800 s at 616 K and 726 K). These results clearly reveal the radiation hardening due to radiation exposure as well the degree of recovery following thermal annealing. These results demonstrate the capability of the SSM system to quantify the degree of embrittlement and recovery due to mitigation procedures of nuclear reactor pressure vessel steels. Furthermore, the SSM system can also monitor, nondestructively in-situ, the re-embrittlement rate of nuclear pressure vessels following their thermal annealing during their life-extension.

Deformation Anisotropy of Zircalloys

Zirconium alloys are extensively used in water reactors as thin-walled tubing to clad highly radioactive fuel [10], and these materials exhibit anisotropic mechanical properties. A thorough knowledge of the mechanical anisotropy of these

materials is a prerequisite in our ability to predict the dimensional changes in-service [11]. In addition, the ease with which the thin-walled cladding is tube-reduced from mother tube (tube shells) is also controlled by the mechanical anisotropy of the starting materials. ABI is suitable for determining the stress-strain behaviors along the three orthogonal directions of the tubing: axial, hoop and thickness. Figure 8 depicts the indentation stress versus strain curves obtained along the thickness (r), axial (z) and hoop (θ) directions of a thin-walled (~0.69 mm) Zircaloy-4 tubing. We note the distinct differences between the mechanical properties along the three orthogonal directions. It is possible to derive the mechanical anisotropy parameters from these data [12]. However, the anisotropic nature of deformation makes it complex to correlate the multiaxial indentation to uniaxial tension, and further research is required.

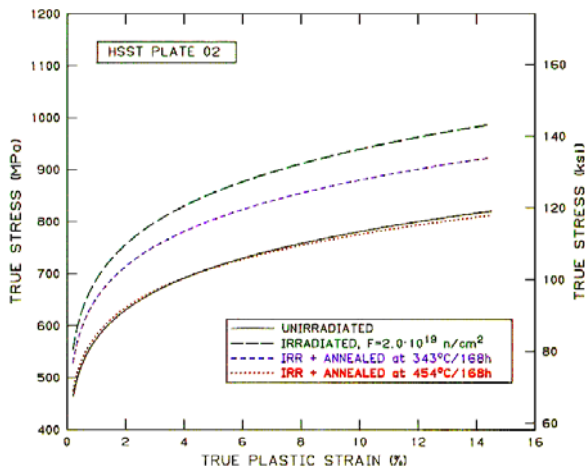


Figure 7

ABI Data on A533B Steel - Effect of Radiation and Annealing

Strain-Rate- Sensitivity (SRS) of Sn5 % Sb Solder

Sn5%Sb is one of the materials being considered as lead-free solder replacements in semiconductor electronic packaging applications [13, 14]. There is a dire need to develop techniques to characterize the mechanical, creep and fatigue properties on the solder structures so that these properties can be gleaned in the *real* situations where the amounts of material available are very small and thus the properties could be different from bulk. Conventional tensile creep tests were performed at room temperature from which the strain-rate variation with stress is investigated. We used SSM to obtain load-depth curves in single cycle mode at varied indenter speeds from which the strain-rates were calculated,

$$\dot{\epsilon} \approx \frac{2}{5} \frac{v_i}{d_p} \quad (10)$$

where v_i is the indenter velocity and d_p is the plastic indenter diameter at the point of interest. The corresponding true ultimate tensile stress was calculated using equations given earlier. Figure 9 depicts the influence of strain-rate on the load depth curves, and double-log plots of stress versus strain-rate (the slopes yield inverse of the SRS) are shown in Fig. 10

where the ABI results are plotted along with the creep data. We see an excellent correlation between them.

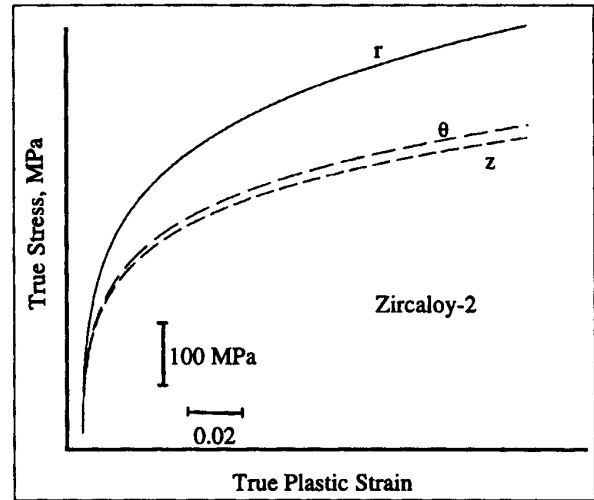


Figure 8

ABI-Derived Stress-Strain Curves for Zircaloy Cladding Depicting Mechanical Anisotropy

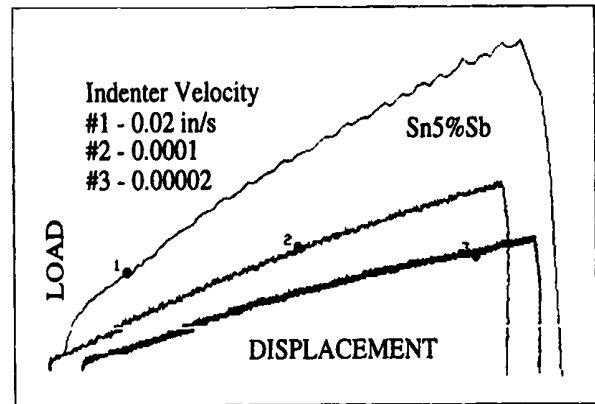


Figure 9

Indentation Load vs Depth Curves (Sn5%Sb)

The low stress ($\sigma \leq 1.23 \times 10^{-3} E$) data follow a power-law (Norton) creep,

$$\dot{\epsilon} = A_I \sigma^{4.5} \quad (11a)$$

while at high stresses, the strain-rate increased exponentially with stress,

$$\dot{\epsilon} = A_H e^{B'\sigma} = A_H e^{0.182\sigma}, \sigma \text{ in psi.} \quad (11b)$$

Thus the strain-rate-sensitivity ($m = \frac{d \ln \sigma}{d \ln \dot{\epsilon}}$) is 0.222 at low

stresses while it decreases with stress at high stresses. The critical stress for the transition from power-law creep to exponential stress region is commonly referred to as the power-law breakdown, and the present value of $1.23 \times 10^{-3} E$ is in close agreement with creep data on many pure metals and alloys [15]. These results make it possible to derive the activation area for the deformation process and thus make it

feasible to identify the underlying micromechanism. Details of these analyses may be found elsewhere [14, 16].

An overlap at low stresses corresponding to ABI tests with the creep tests is also apparent albeit only a few creep tests could be performed at these very high strain-rates. In addition to the fact that the ABI test results are in excellent agreement with creep, these tests took about three hours time while they cover more than three orders of magnitude while the creep tests were performed for a long period in excess of four months. Due to extremely short durations involved in obtaining high strain-rate / stress data, conventional creep tests are not practical. Moreover, only one sample could be used to obtain this type of information using ABI/SSM.

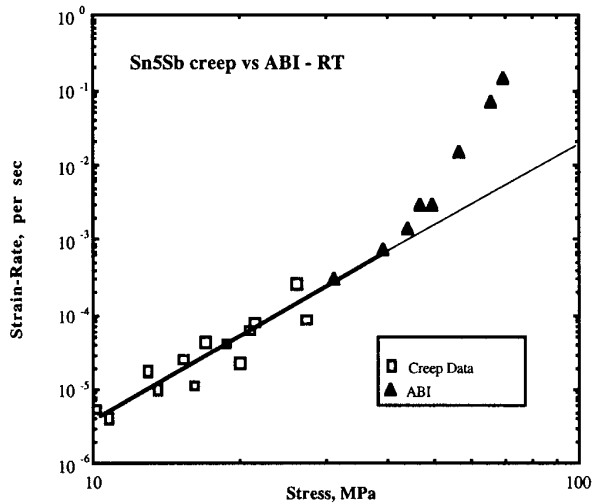


Figure 10
Correlation of ABI and Creep Results for Sn5%Sb

Summary

ABI is a relatively simple technique to characterize flow and creep properties of materials used in various applications, and we demonstrated its success in determining these properties of various structural metals (ferritic steels, stainless steels, Zircalloys, electronic solders) and their welds and HAZs. The SSM system quantified the degree of neutron-embrittlement damage as well as the percentage recovery in mechanical properties resulting from post-irradiation thermal annealing of nuclear pressure vessel steels. Furthermore, welding and repair procedures can be accurately assessed. Compared to conventional tests, ABI technique has many advantages: small amounts of material are adequate, no extensive specimen preparation is necessary, extensions to *in-situ* tests on *real* structures can be made and thus the method is useful in monitoring in-service mechanical property changes; monitor the aging of bridges and other critical components and to verify their structural integrity.

References

1. D. Tabor, *The Hardness of Metals*, Oxford University Press, New York (1951).

2. F. M. Haggag, *Field Indentation Microprobe for Structural Integrity Evaluation*, U.S. Patent No. 4,852,397, August 1, 1989.
3. F. M. Haggag, "In-Situ Measurements of Mechanical Properties Using Novel Automated Ball Indentation System," in *Small Specimen Test Techniques Applied to Nuclear Reactor Thermal Annealing and Plant Life Extension*, ASTM STP 1204, W. R. Corwin, F. M. Haggag, and W. L. Server, Eds., American Society for Testing and Materials, Philadelphia (1993) pp. 27-44.
4. F. M. Haggag, et al., "Use of Automated Ball Indentation Testing to Measure Flow Properties and Estimate Fracture Toughness in Metallic Materials," in *Applications of Automation Technology to Fatigue and Fracture Testing*, ASTM STP 1092, A. A. Braun, N. E. Ashbaugh, and F. M. Smith, Eds., American Society for Testing and Materials, Philadelphia (1990) pp. 188-208.
5. F.M. Haggag, et al., "The Use of Field Indentation Microprobe in Measuring Mechanical Properties of Welds," in *Recent Trends in Welding Science and Technology, TWR '89, Proceedings of the 2nd International Conference on Trends in Welding Research*, ASM (1990) pp. 843-849.
6. Haggag, F. M., "Application of Flow Properties Microprobe to Evaluate Gradients in Weldment Properties," in *Proceedings of the ASM 3rd International Conference on Trends in Welding Research*, ASM (1992) pp. 629- 635.
7. S.G. Druce, G. Gage and W.J. Phythian, "The Use of Miniature Specimen Techniques for the Assessment of Material Condition," *PVP Vol. 252, ASME* (1993) pp. 51 - 66.
8. Haggag, F. M. and Bell, G. E. C., "Measurement of Yield Strength and Flow Properties in Spot Welds and Their HAZs at Various Strain Rates," in *Proceedings of the ASM 3rd International Conference on Trends in Welding Research*, ASM (1992) pp. 637 - 642.
9. F. M. Haggag, et al., "Use of Portable / In-Situ SSM System to Measure Stress-Strain Behavior and Damage in Metallic Materials and Structures," in *Nontraditional Methods of Sensing Stress, Strain, and Damage in Materials and Structures*, ASTM STP 1318, G. Lucas and D. Stubbs, Eds., American Society for Testing and Materials, Philadelphia (1996) in print.
10. K.L. Murty, "Technological Applications of Crystallographic Textures of Zirconium Alloys," *Materials Forum*, Institute of Metals and Materials Australasia Ltd., 15 (1991) pp. 217 - 230.
11. K.L. Murty, "Biaxial Creep Behavior of Textured Zircaloy Tubing," *Journal of Metals*, Feb. 1992, pp. 49-55.
12. K.L. Murty, "Mechanical Anisotropy of Textured Zircaloy TREX Using Impression Testing," in *Proceedings of J.C.M. Li Symposium on Mechanics of Advanced Materials*, TMS (S.N.G. Chu et al., eds.) 1995, pp. 245 253.
13. R.K. Mahidhara, et al., "Room Temperature Tensile Properties of Sn-5%Pb Solder," *J. Mat. Sci. Lets.*, 13 (1994) pp. 1387-1389.
14. K.L. Murty and F.M. Haggag, "Characterization of Strain-Rate Sensitivity of Sb-5%Sn Solder using ABI Testing," in *Proceedings of Second International Conference on Microstructures and Mechanical Properties of Aging Materials*, P.K. Liaw et al, eds, TMS, in print.